# Integration of dual-source dual-energy CT quantitative parameters and ultrasound image features: A diagnostic method for extraglandular invasion of papillary thyroid carcinoma

MUHAMMAD ASAD IQBAL[1,2*], NIDA FATIMA MOAZZAM[1*], HUI ZHOU[1*], JIE HOU[1], HUI SUN[3], DONGGANG PAN[4] and XIAN WANG[2]

[1]School of Medicine, Jiangsu University, Zhenjiang, Jiangsu 212013, P.R. China; [2]Department of Ultrasound, Affiliated People's Hospital of Jiangsu University, Zhenjiang, Jiangsu 212050, P.R. China; [3]Department of Pathology, Affiliated People's Hospital of Jiangsu University, Zhenjiang, Jiangsu 212050, P.R. China; [4]Department of Radiology, Affiliated People's Hospital of Jiangsu University, Zhenjiang, Jiangsu 212050, P.R. China

Received December 3, 2024; Accepted April 1, 2025

DOI: 10.3892/ol.2025.15102

**Abstract.** The present study explored the impact of dual-source dual-energy CT (DECT) quantitative parameters combined with ultrasonography (US) imaging features on the diagnostic value of extrathyroidal extension in papillary thyroid carcinoma (PTC). Analysis was conducted on 136 nodules pathologically confirmed as PTCs in 102 patients who presented to the Affiliated People's Hospital of Jiangsu University (Zhenjiang, China) between January 2018 and August 2023. All patients underwent DECT and US examinations, and the parameters for nodule examination using DECT included iodine concentration, normalized iodine concentration and energy spectrum curve slope. Gemstone spectral imaging (GSI) and US imaging features of extrathyroidal extension (ETE) and non-ETE groups were statistically examined for diagnostic usefulness. A logistic regression model was then constructed and diagnostic performance was assessed using receiver operating characteristics curves. The area under the curve (AUC) for iodine concentration in identifying ETE was 0.722, with the highest accuracy when 2.88 mg/ml was used as the diagnostic threshold. The corresponding sensitivity and specificity were 58.3 and 85.6%, respectively, with a Youden index of 0.44. The AUC for normalized iodine concentration in identifying ETE was 0.713, with the highest accuracy when 0.285 was used as the diagnostic threshold. The corresponding sensitivity and specificity were 65.7 and 78.6%, respectively, with a Youden index of 0.443. The AUC for slope of Hounsfield unit curve in identifying ETE was 0.738, with the highest accuracy when 3.4 was used as the diagnostic threshold. The corresponding sensitivity and specificity were 68.5 and 78.6%, respectively, with a Youden index of 0.471. The AUC of US (maximum longitudinal diameter >5 mm) was 0.712, with the highest accuracy when 3.845 cm was used as the diagnostic threshold. The corresponding sensitivity and specificity were 46.3 and 89.3%, respectively, with a Youden index of 0.356. The AUC for ETE identification using GSI and US morphological parameters was 0.782, with the highest accuracy when 0.762 was used as the diagnostic threshold. The corresponding sensitivity and specificity were 80.6 and 85.7%, respectively, with a Youden index of 0.663. In conclusion, the accuracy of ultrasound combined with GSI parameters in diagnosing ETE of PTC was improved when compared with that of single DECT and ultrasound morphological examinations.

*Correspondence to:* Dr Donggang Pan, Department of Radiology, Affiliated People's Hospital of Jiangsu University, 8 Dianli Road, Zhenjiang, Jiangsu 212050, P.R. China
E-mail: dongzi1125@aliyun.com

Dr Xian Wang, Department of Ultrasound, Affiliated People's Hospital of Jiangsu University, 8 Dianli Road, Zhenjiang, Jiangsu 212050, P.R. China
E-mail: wangxian8812@126.com

*Contributed equally

*Key words:* papillary thyroid carcinoma, extraglandular invasion, metastasis, dual-energy CT, ultrasonography

## Introduction

Thyroid cancer is the most common malignancy of the endocrine system; >90% of the pathological types are papillary thyroid carcinomas (PTC) and ~80% of patients with PTC have a good prognosis. However, in patients with invasion of the trachea, esophagus, recurrent laryngeal nerve and large blood vessels, the 10-year survival rate decreases to 26% (1,2). Several factors have been used to evaluate the malignancy, prognosis, possibility of postoperative metastasis and recurrence of PTC before surgery. Commonly used clinical factors include the age, grade, tumor invasion and tumor size (AGES), and age and tumor invasion (AEMS) systems. Additionally, tumor extent, distant metastasis, tumor size and extrathyroidal extension (ETE) are considered to be independent risk factors for thyroid cancer (3-5). An ETE indicates that a tumor is highly aggressive and has a significant likelihood of spreading

to distant parts of the body (6-8). The TNM staging system for thyroid cancer has been outlined in the 7 and 8th editions of the American Joint Committee on Cancer (2,9). ETE can be categorized as follows: i) Microscopic ETE (histology, band muscle invasion; and ii) gross ETE, band muscle invasion and more serious external invasion (subcutaneous tissue, major organs, nerves and blood vessels) (9).

An accurate preoperative assessment of ETE in PTC is crucial for clinicians to develop optimal therapeutic strategies that are both individualized and evidence-based (10-13). The implementation of appropriate surgical interventions (including total/subtotal thyroidectomy and thyroid isthmusectomy) combined with adjuvant therapies (such as thyrotropin suppression, radioactive iodine therapy, chemotherapy, external beam radiation and chemical embolization) has been demonstrated to significantly reduce postoperative recurrence rates, enhance patient survival outcomes and improve quality of life indicators (14,15).

Currently, imaging methods for the preoperative diagnosis of ETE in PTC mainly include ultrasonography (US) and computed tomography (CT) scans. US is the preferred imaging method for the diagnosis of PTC. US is simple, non-invasive, inexpensive and reproducible in real-time. However, US fails to accurately represent the spatial relationship between PTC and the surrounding trachea and esophagus, and there is still a certain degree of false-positive and false-negative rates in the preoperative evaluation of ETE (16). The radiation-hardening effect in traditional CT imaging causes the absorption coefficient of X-rays by the nodules to no longer be constant. This change leads to a change in the average energy of the X-rays, which in turn causes problems such as information loss, hardening artifacts and inaccurate CT value measurements (17-19). Dual-energy CT (DECT) imaging can generate material decomposition (MD) images using monochromatic images with photon energies varying from 40 to 140 keV. These images were then used to create spectral Hounsfield unit (HU) curves. The inclusion of molecular dynamics images and spectral HU curves is beneficial for identifying ETE of PTC (20,21). Therefore, the present study aimed to explore the diagnostic value of DECT combined with US for detecting ETE in PTC.

## Materials and methods

*Research participants.* Between January 2018 and August 2023, 102 patients with pathologically confirmed PTC (comprising 136 nodules) who were hospitalized in Affiliated People's Hospital of Jiangsu University (Zhenjiang, China) for surgery, were all examined using US and DECT prior to surgery. The patient cohort included 69 female and 33 male patients, aged 21-72 years old (mean ± SD age, 47.14±10.73 years). The male-to-female ratio was ~1:2.09; 62 patients (60.7%) were aged >45 years old and 40 patients (39.3%) were ≤45 years old. Asymptomatic physical examination was used in 74 cases, demonstrating: 12 cases of neck swelling, 4 cases of dysphagia, 5 cases with symptoms of oppression and 7 cases of hoarseness. The present study was approved by the Institutional Ethical Review Committee of Jiangsu University Affiliated People's Hospital (approval no. K-20170104-Y; Zhenjiang, China) and all the patients provided written informed consent.

The inclusion criteria were as follows: i) Age, ≥18 years; ii) postoperative pathological confirmation of PTC; iii) absence of any history of neck tumors other than thyroid tumors; and iv) absence of neck radiation therapy. The exclusion criteria were as follows: i) Benign thyroid tumors confirmed according to postoperative pathology; and ii) malignant tumors other than PTC confirmed using pathology.

*Instruments and methods*

*US inspection methods.* The equipment used in the present study was a Q5 color Doppler ultrasound diagnostic system (System Software 3.2.1; Philips Healthcare) equipped with a linear array high-frequency probe operating at 5-12 MHz. The system was configured with the pre-set 'Thyroid' examination mode for optimal imaging. Before the examination, the patient assumed a supine position, with the head removed from the headrest and the neck slightly inclined back to maximize neck exposure. The conditions preprogrammed into the thyroid examination instrument were used. Longitudinal and cross-sectional analyses were performed by positioning the instrument beneath the thyroid cartilage.

The thyroid diameter was routinely measured in the superficial thyroid deep muscle group, trachea, esophagus and large vessels. Additionally, the primary lesion, location, internal echo, aspect diameter ratio, blood flow signal, morphology, boundary, calcification, elasticity and cervical lymph node characteristics, including maximum diameter, shape, edge, calcification, cystic degeneration, lymphatic hilus structure and blood flow signal, were measured.

*CT examination method.* The present study used a third-generation DECT scanner (Siemens AG) to perform dual-energy scans of the cervical arteries and veins with the patient's neck extended in the supine position. The third-generation DECT scanner (Siemens AG) adopted a dual-source configuration with two X-ray tubes and corresponding detectors, which could work simultaneously at different energy levels to collect dual-energy data in a single scan. The present scan range extended from the cranium base to the aortic arch. Dual-energy scanning was used to scan the arterial and venous phases. The fusion coefficients for high and low tube voltage images were set to 0.3, respectively, with exposure parameters of 89 mAs, collimator width of 128x0.6 mm, matrix dimensions of 256x256 and pitch of 0.7 were the scanning parameters. Iopromide (Bayer AG) was used as the contrast agent at a concentration of 1.5 ml/kg and an injection flow rate of 3.5 ml/sec. Using contrast agent bolus monitoring technology, scanning commenced 45 sec following the injection of iopromide. All images containing data files were transferred to a workstation to produce spectral HU curves, iodine-based MD images, and 40, 70 and 100 keV images. These curves were analyzed by a radiologist with 15 years of experience in head and neck cancer diagnosis and imaging measurements. The examination was conducted using gemstone spectral imaging (GSI) viewer image analysis software (Syngo.via; Siemens AG).

An additional radiologist with >10 years of expertise in diagnosing head and neck cancer assessed the CT GSI parameters by analyzing the 70 keV images. A region of interest (ROI) was selected over the lesion to avoid capturing images of necrotic or calcified areas. The parameters were averaged after three measurements. Iodine concentration (IC), normalized IC (NIC) and slope

Table I. Comparison of clinical characteristics of PTC cases in patients without ETE (n=28) and with ETE (n=108).

| Characteristics | Non-ETE | ETE | P-value |
|---|---|---|---|
| Mean age, years | 43.67±14.67 | 47.59±10.06 | 0.069 |
| Sex ratio (Male: female) | 1:1.88 | 1:2.16 | 0.811 |
| Mean tumor diameter, cm | 3.35±1.37 | 3.59±1.97 | 0.524 |
| Tumor site | | | 0.834 |
| Isthmus | 9 | 40 | |
| Left lobe | 11 | 37 | |
| Right lobe | 8 | 31 | |

ETE, extrathyroidal extension.

Table II. Diagnostic value of ultrasonography parameters in diagnosing ETE.

| Lesion morphological characteristics | ETE, n | Non-ETE, n | $\chi^2$ | P-value | Sensitivity, % | Specificity, % | Accuracy, % | Positive predictive value, % | Negative predictive value, % |
|---|---|---|---|---|---|---|---|---|---|
| Contrast enhancement | 72 | 14 | 2.65 | 0.125 | 66.7 | 50.0 | 63.2 | 83.7 | 28.0 |
| Maximum longitudinal diameter >5 mm | 80 | 13 | 7.86 | 0.007 | 74.1 | 53.6 | 69.9 | 86.0 | 34.9 |
| Calcification | 71 | 15 | 1.41 | 0.274 | 65.7 | 46.4 | 61.8 | 82.6 | 26.0 |
| Cystic changes | 54 | 13 | 0.11 | 0.833 | 50.0 | 53.6 | 50.7 | 80.6 | 23.1 |

ETE, extrathyroidal extension.

of HU curve (λHU) in the ROI, CT attenuation value (HU) and IC of the common carotid artery on the same image slice were GSI parameters. The NIC and λHU formulations are expressed as follows: λHU=[CT value (40 keV)-CT value (100 keV)]/(100-40); and $NIC=IC_{ROI}/IC_{common\ carotid\ artery}$. 'CT value (40 keV)' and 'CT value (100 keV)' represented the measurements of CT attenuation at energy levels of 40 and 100 keV, respectively.

*Image analysis method*. The US and DECT data of all selected PTCs were analyzed in a blinded manner by two attending or the aforementioned ultrasound imaging and radiology doctors to determine whether the PTC contacted the thyroid capsule and whether there was an invasion of the adjacent organs. In cases of disagreement, consensus was reached. The final results were based on surgical records and pathological results.

The image criteria for preoperative US and DECT diagnosis of ETE were: i) The lesion protruded from the thyroid capsule, and invaded the sternothyroid muscle and soft tissue surrounding the thyroid or it contacts the thyroid capsule by >25%; and ii) in addition to the thyroid capsule, the lesion spread to the larynx, trachea, esophagus, recurrent laryngeal nerve, carotid artery and mediastinal blood vessels (2-4,22-24).

*Pathological diagnosis methods*. Fresh tissue samples were fixed in formalin at room temperature and prepared by standardized procedures of gradient ethanol dehydration, xylene transparency, and paraffin embedding. The embedded tissue was cut into 4-$\mu$m tissue sections using a microtome. The cells were deparaffinized with xylene and rehydrated through gradient ethanol. In the staining process, the nuclei were stained with hematoxylin solution at room temperature for 5-6 min to make the nuclei blue, and then differentiated with hydrochloric acid and rinsed with running water to enhance the contrast. The cytoplasm was then counterstained with eosin staining solution for another 10 sec at room temperature to give a pink color. Finally, sections were dehydrated with gradient ethanol, made transparent with xylene, and sealed with neutral gum for visualization under a light microscope.

*Statistical analysis*. All data were statistically analyzed using the SPSS Statistics (version 20.0; IBM Corp.). The measurement data following a normal distribution were expressed as mean ± standard deviation, using independent sample t-test. Contrast enhancement, maximum longitudinal diameter >5 mm, calcification and cystic changes were analyzed using the $\chi^2$ test. Continuous data were converted into categorical data, and the cut-off values established by receiver operating characteristic (ROC) curve analysis were used to analyze the IC, NIC and λHU variables. The area under the curve (AUC) was calculated and the diagnostic boundary point of Young's modulus was determined according to the highest critical point of Youden index. $P<0.05$ was considered to indicate a statistically significant difference.

Table III. Diagnostic value of gemstone spectral imaging parameters in diagnosing ETE.

| Spectral imaging parameters | ETE (n=108) | Non-ETE (n=28) | t | P-value |
|---|---|---|---|---|
| IC, mg/ml | 3.09±1.24 | 2.53±0.88 | -2.3 | <0.001 |
| NIC | 0.41±0.21 | 0.27±0.20 | -3.3 | 0.001 |
| λHU, HU/keV | 3.94±1.61 | 2.87±0.93 | -3.4 | <0.001 |

ETE, extrathyroidal extension; IC, iodine concentration; NIC, normalized IC; HU, Hounsfield unit; λHU, slope of HU curve.

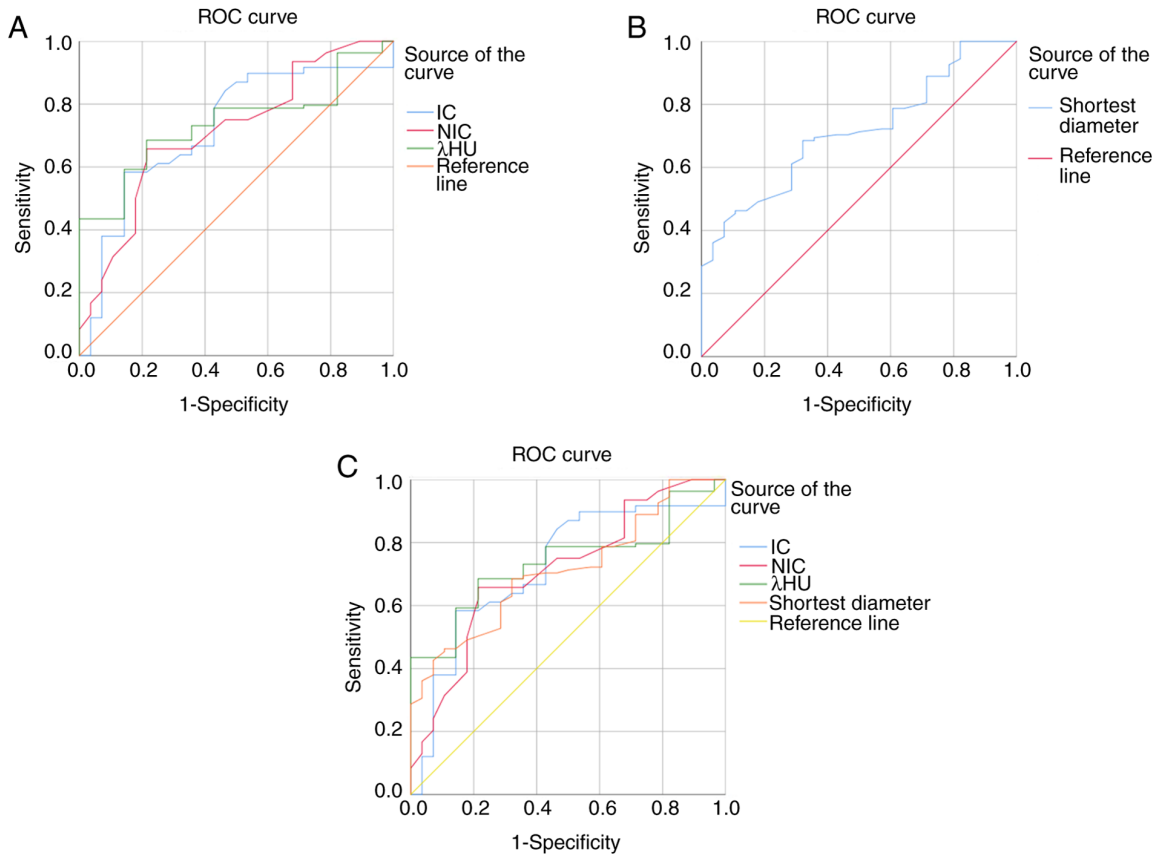


Figure 1. ROC curve of dual-energy CT and ultrasound diagnosis. (A) ROC curve using IC, NIC and λHU parameters in combination to diagnose ETE. (B) ROC curve using US morphological parameters to diagnose ETE. (C) ROC curve using IC, NIC and λHU parameters and US morphological parameters in combination to diagnose ETE. ROC, receiver operating characteristic; US, ultrasonography; ETE, extrathyroidal extension; IC, iodine concentration; NIC, normalized IC; HU, Hounsfield unit; λHU, slope of HU curve.

## Results

*Comparison of clinical characteristics between ETE and non-ETE cases*. Between January 2018 and August 2023, surgical resection was performed on all 102 PTC cases (comprising 136 nodules) in the present cohort, with pathological confirmation obtained. DECT and US were performed preoperatively. A total of 136 lesions were observed, comprising 49 lesions on the isthmus, 39 on the right side and 48 on the left side; diameters ranged from 0.4 to 10.5 cm (mean diameter, 3.57±1.91 cm). A comparison of the clinical characteristics of the patients with and without ETE is presented in Table I. Age, sex and tumor diameter did not significantly differ between patients with and without ETE (P>0.05).

*Comparison of the diagnostic value of US and DECT for ETE in PTC*. The sensitivity, specificity and accuracy of GSI parameters (IC, NIC and λHU) and US morphological parameters (contrast enhancement, maximum longitudinal diameter, calcification and cystic change) in diagnosing ETE are shown in Tables II and III. Through the analysis of the GSI parameters (IC, NIC and λHU) of the lesions, the optimal threshold, sensitivity, specificity and accuracy of GSI parameters for diagnosing ETE were determined. The IC, NIC and λHU of the ETE group were significantly increased compared with those of the non-ETE group (P<0.001).

*ROC curve analysis of DECT parameters and US combined diagnosis of ETE*. The AUC for IC in identifying ETE was 0.722, with the highest accuracy when 2.88 mg/ml was used

Table IV. Comparison of IC, NIC and λHU parameter diagnostic ETE AUC curves.

| Test result variables | Area | Standard error[a] | Asymptotic sig[b] | Asymptotic 95% confidence interval |
|---|---|---|---|---|
| IC | 0.722 | 0.054 | 0.000 | 0.616-0.828 |
| NIC | 0.713 | 0.054 | 0.001 | 0.607-0.819 |
| λHU | 0.738 | 0.044 | 0.000 | 0.652-0.824 |

[a]Under the non-parametric assumption. [b]Null hypothesis, true area=0.5. ETE, extrathyroidal extension; IC, iodine concentration; NIC, normalized IC; HU, Hounsfield unit; λHU, slope of HU curve.

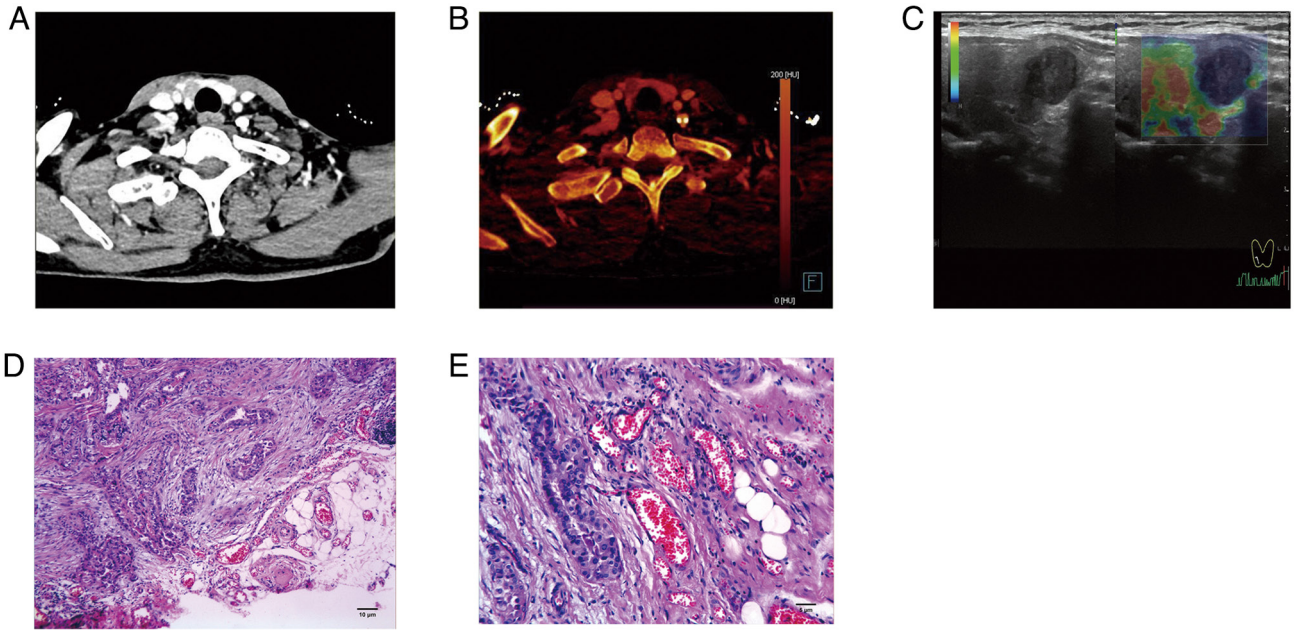


Figure 2. Representative images of malignant thyroid nodules. (A and B) Representative enhanced typical images, showing an oval-shaped localized iodine deficiency area in the RL of the thyroid gland with clear boundaries and uneven density. (C) Conventional and elastic ultrasound, showing a hypoechoic mass in the RL of the thyroid gland with clear boundaries and uneven internal echo, elasticity score: 3 points. (D and E) Representative pathology images showing papillary thyroid cancer invading the thyroid capsule. Hematoxylin and eosin staining [scale bar, (D) 10 and (E) 5 $\mu$m]. RL, right lobe.

as the diagnostic threshold. The corresponding sensitivity and specificity were 58.3 and 85.6%, respectively, with a Youden index of 0.44. The AUC of NIC in identifying ETE was 0.713, with the highest accuracy when 0.285 was used as the diagnostic threshold. The corresponding sensitivity and specificity were 65.7 and 78.6%, respectively, with a Youden index of 0.443. The AUC of λHU in identifying ETE was 0.738, with the highest accuracy when 3.4 was used as a diagnostic threshold. The corresponding sensitivity and specificity were 68.5 and 78.6%, respectively, with a Youden index of 0.471 (Fig. 1A). The AUC of US (maximum longitudinal diameter >5 mm) morphological parameters for identifying ETE was 0.712, with the highest accuracy when 3.845 cm was used as the diagnostic threshold. The corresponding sensitivity and specificity were 46.3 and 89.3%, respectively, with a Youden index of 0.356 (Fig. 1B). The differences between the two groups were statistically significant (Table IV).

The AUC of the GSI parameters combined with the US morphological parameters to identify ETE was 0.782, with the highest accuracy when 0.762 was used as the diagnostic threshold. The corresponding sensitivity and specificity were 80.6 and 85.7%, respectively, with a Youden index of 0.663 (Fig. 1C).

The GSI and US morphological parameters were combined to diagnose ETE in patients with PTC differentially. Among them, IC >2.88 mg/ml, NIC >0.285, λHU >3.4, and a lesion that contacts the thyroid capsule >25% and protrudes from the thyroid capsule indicated ETE (Fig. 2).

## Discussion

ETE is an important factor affecting PTC prognosis; the American Thyroid Association guidelines (25) indicate that for patients with PTC without clinical evidence of ETE, only lobectomy and isthmusectomy are necessary. Therefore, an accurate preoperative assessment of the presence of ETE can guide surgeons in choosing a reasonable and standardized treatment plan that is of significant clinical importance.

US is the preferred imaging modality for diagnosing PTC (26,27). US offers high resolution and is radiation-free, allowing clear visualization of PTC boundaries. However, US is highly dependent on the operator's skill, which can lead

to reduced objectivity in diagnosis owing to human factors. Additionally, US has certain limitations in displaying lymph nodes in the retropharyngeal and parapharyngeal spaces and the thyroid capsule. However, DECT can generate quantitative parameters such as monoenergetic and MD images based on the differing X-ray absorption coefficients of various substances. These findings provide a theoretical basis for the disease diagnosis. DECT offers enhanced tissue contrast information, accurately displaying the size, extent, location, potential extrathyroidal extension, lymph node metastasis and the relationship with the surrounding tissues and organs of PTC (17,28-30). Consequently, the application of DECT for thyroid lesions has increased in recent years (30).

The findings of the present study indicated that a maximum longitudinal diameter >5 mm in ultrasound features has significant clinical implications for predicting ETE in PTC. This phenomenon may be attributed to differences in the biological behavior of PTC. During the early stages of PTC, cancer cells in the anterior-posterior direction are in the proliferative phase, whereas those in other directions remain relatively quiescent. This results in a larger diameter in the anteroposterior direction compared with that in the lateral direction. Additionally, when the maximum longitudinal diameter of a PTC >5 mm, the tumor is more likely to exhibit a vertical growth pattern; this growth pattern increases the risk of capsular invasion in PTC (31,32).

Vaish *et al* (33) used histological results as the gold standard to calculate the sensitivity, specificity, negative and positive predictive value, and accuracy of US, CT and US + CT in detecting the overall, lateral compartment and central compartment regional metastasis. It was found that CT has higher sensitivity in detecting lymph node metastasis. CT can be used to complement US to address the issue of low specificity. The present study used pathological results as the 'gold standard' and combined DECT with ultrasound image features to diagnose ETE in PTC. Compared with traditional CT, which mainly relies on morphological features, DECT uses two different energies of X-rays simultaneously to analyze the attenuation differences of substances at different energies, thereby accurately distinguishing tissue components. Meanwhile, compared with the study by Vaish *et al* (33), the present study added two quantitative indicators, IC and NIC, which objectively reflect the uptake of iodinated contrast agents by PTC and indirectly evaluate the angiogenesis status of the lesion area. The present study also included the characteristic parameter λHU of the organization, which represents the differences in physical density and chemical composition among different tissues (34). Therefore, IC, NIC and λHU can help diagnose PTC with or without ETE.

The present study further demonstrated that the PTC group with ETE exhibits significantly increased IC, NIC and λHU values in both the arterial and venous phases compared with that the non-ETE group, which suggested that the PTC group with ETE has an increased iodine uptake. This could be attributed to the ability of DECT to depict characteristic spectral curves based on CT values at different unit quantities and to reflect local lesions and microvascular perfusion through the slope of the spectral curve. Because the tissue structures of PTC with metastatic and non-metastatic ETE differ, their X-ray absorption coefficients vary, leading to different slopes of the spectral curve. The amount and capacity of iodine uptake by cells are closely related to the blood supply (16,34). PTC with ETE contained more neovascularization and a richer blood supply (35), resulting in a higher iodine uptake rate and significant enhancement in the early phase of contrast, whereas the PTC group without ETE had a lower iodine uptake rate. Additionally, the diagnostic efficacy of the quantitative parameters in both the arterial and venous phases of ETE was high, further confirming the significant diagnostic value of DECT quantitative parameters in the ETE of PTC.

In the present study, the AUC of DECT combined with GSI parameters and ultrasound morphological parameters for distinguishing ETE was 0.782, which was higher in comparison with the AUC of IC, NIC and λHU. The diagnostic efficiency of DECT was increased compared with that of single-parameter diagnosis. As ultrasound can clearly display the boundaries of the PTC, DECT has excellent soft-tissue contrast and quantitative analysis capabilities, and is advantageous in evaluating the thyroid envelope and deep tissue (36,37). DECT and ultrasound could complement each other in evaluating the ETE of PTC, and their combined use can significantly improve diagnostic accuracy and comprehensively evaluate the invasiveness of PTC.

The present study had limitations: i) this was a single-center study with small sample size; and ii) the recurrence rate after PTC surgery was not included in the present study. Further research includes the incorporation of the recurrence rate of PTC and future large-scale clinical studies to provide more data for the diagnosis of ETE in PTC.

In conclusion, the diagnostic accuracy of GSI parameters combined with ultrasound morphology parameters was superior to that of solitary DECT and ultrasound morphology examination when identifying ETE in PTC. Integrating dual-source DECT quantitative parameters and ultrasound image features can improve the diagnostic accuracy of extraglandular invasion in PTC. Clinicians can potentially enhance preoperative staging and treatment planning for patients diagnosed with PTC using sophisticated imaging methodologies, artificial intelligence algorithms and molecular markers. Such advancements could potentially result in improved patient outcomes and individualized management approaches in the future.

**Acknowledgements**

Not applicable.

**Funding**

The present study received contributions from the Jiangsu Provincial Health Commission Scientific Research Project (grant no. Z2021071), Zhenjiang City Key R&D Plan-Social Development (grant no. SH2023049), Jiangsu University Medical Education Collaborative Innovation Fund (grant no. JDYY2023015) and Jiangsu University's 22nd batch of college student scientific research projects (grant no. 22A485).

**Availability of data and materials**

The data generated in the present study are not publicly available due to confidential patient information and privacy concerns but may be requested from the corresponding author.

## Authors' contributions

MAI, NFM and HZ designed the study framework and wrote the original manuscript. JH and HS conducted data collection and data analysis. DP and XW analyzed and interpreted data results, and critically modified the manuscript for important intellectual content. All authors collaborated in writing the manuscript and critically reviewed its content. DP and XW confirm the authenticity of all the raw data. All authors read and approved the final version of the manuscript.

## Ethics approval and consent to participate

The present study was conducted in compliance with ethical standards and was approved by the Ethics Committee of Jiangsu University Affiliated People's Hospital (approval no. K-20170104-Y; Zhenjiang, China). All participants provided written informed consent before their inclusion in the present study.

## Patient consent for publication

Written informed consent for the publication of their anonymized data was obtained from all patients involved in the present study. No identifiable patient information is included in the present study.

## Competing interests

The authors declare that they have no competing interests.

## References


1. Siegel RL, Miller KD and Jemal A: Cancer statistics, 2019. CA Cancer J Clin 69: 7-34, 2019.
2. Tran B, Roshan D, Abraham E, Wang L, Garibotto N, Wykes J, Campbell P and Ebrahimi A: An analysis of the american joint committee on cancer 8th edition T staging system for papillary thyroid carcinoma. J Clin Endocrinol Metab 103: 2199-2206, 2018.
3. Hay ID, Johnson TR, Thompson GB, Sebo TJ and Reinalda MS: Minimal extrathyroid extension in papillary thyroid carcinoma does not result in increased rates of either cause-specific mortality or postoperative tumor recurrence. Surgery 159: 11-19, 2016.
4. Chen W, Zheng R, Baade PD, Zhang S, Zeng H, Bray F, Jemal A, Yu XQ and He J: Cancer statistics in China, 2015. CA Cancer J Clin 66: 115-132, 2016.
5. Haugen BR: 2015 American thyroid association management guidelines for adult patients with thyroid nodules and differentiated thyroid cancer: What is new and what has changed? Cancer 123: 372-381, 2017.
6. Youngwirth LM, Adam MA, Scheri RP, Roman SA and Sosa JA: Extrathyroidal extension is associated with compromised survival in patients with thyroid cancer. Thyroid 27: 626-331, 2017.
7. Chu KP, Baker S, Zenke J, Morad A, Ghosh S, Morrish DW, McEwan AJBS, Williams DC, Severin D and McMullen TPW: Low-activity radioactive iodine therapy for thyroid carcinomas exhibiting nodal metastases and extrathyroidal extension may lead to early disease recurrence. Thyroid 28: 902-912, 2018.
8. Liu L, Oh C, Heo JH, Park HS, Lee K, Chang JW, Jung SN and Koo BS: Clinical significance of extrathyroidal extension according to primary tumor size in papillary thyroid carcinoma. Eur J Surg Oncol 44: 1754-1759, 2018.
9. Edge SB and Compton CC: The American joint committee on cancer: The 7th edition of the AJCC cancer staging manual and the future of TNM. Ann Surg Oncol 17: 1471-1474, 2010.
10. Lee CY, Kim SJ, Ko KR, Chung KW and Lee JH: Predictive factors for extrathyroidal extension of papillary thyroid carcinoma based on preoperative sonography. J Ultrasound Med 33: 231-238, 2014.
11. Gweon HM, Son EJ, Youk JH, Kim JA and Park CS: Preoperative assessment of extrathyroidal extension of papillary thyroid carcinoma: comparison of 2- and 3-dimensional sonography. J Ultrasound Med 33: 819-825, 2014.
12. Seo YL, Yoon DY, Lim KJ, Cha JH, Yun EJ, Choi CS and Bae SH: Locally advanced thyroid cancer: Can CT help in prediction of extrathyroidal invasion to adjacent structures? AJR Am J Roentgenol 195: W240-W244, 2010.
13. Zhao Y, Li X, Li L, Wang X, Lin M, Zhao X, Luo D and Li J: Preliminary study on the diagnostic value of single-source dual-energy CT in diagnosing cervical lymph node metastasis of thyroid carcinoma. J Thorac Dis 9: 4758-4766, 2017.
14. Tian T, Qi Z, Huang S, Wang H and Huang R: Radioactive iodine therapy decreases the recurrence of intermediate-risk PTC with low thyroglobulin levels. J Clin Endocrinol Metab 108: 2033-2041, 2023.
15. Byrd JK, Yawn RJ, Wilhoit CS, Sora ND, Meyers L, Fernandes J and Day T: Well differentiated thyroid carcinoma: Current treatment. Curr Treat Options Oncol 13: 47-57, 2012.
16. Chen M, Jiang Y, Zhou X, Wu D and Xie Q: Dual-energy computed tomography in detecting and predicting lymph node metastasis in malignant tumor patients: A comprehensive review. Diagnostics (Basel) 14: 377, 2024.
17. García-Figueiras R and Baleato-González S: Quantitative multi-energy CT in oncology: State of the art and future directions. Eur J Radiol 182: 111840, 2025.
18. García-Figueiras R, Oleaga L, Broncano J, Tardáguila G, Fernández-Pérez G, Vañó E, Santos-Armentia E, Méndez R, Luna A and Baleato-González S: What to expect (and what not) from dual-energy CT imaging now and in the future? J Imaging 10: 154, 2024.
19. Haase V, Hahn K, Schöndube H, Stierstorfer K, Maier A and Noo F: Single-material beam hardening correction via an analytical energy response model for diagnostic CT. Med Phys 49: 5014-5037, 2022.
20. Su GY, Xu XQ, Zhou Y, Zhang H, Si Y, Shen MP and Wu FY: Texture analysis of dual-phase contrast-enhanced CT in the diagnosis of cervical lymph node metastasis in patients with papillary thyroid cancer. Acta Radiol 62: 890-896, 2021.
21. Deng Y, Soule E, Samuel A, Shah S, Cui E, Asare-Sawiri M, Sundaram C, Lall C and Sandrasegaran K: CT texture analysis in the differentiation of major renal cell carcinoma subtypes and correlation with Fuhrman grade. Eur Radiol 29: 6922-6929, 2019.
22. Liu X, Ouyang D, Li H, Zhang R, Lv Y, Yang A and Xie C: Papillary thyroid cancer: dual-energy spectral CT quantitative parameters for preoperative diagnosis of metastasis to the cervical lymph nodes. Radiology 275: 167-176, 2015.
23. Kim E, Park JS, Son KR, Kim JH, Jeon SJ and Na DG: Preoperative diagnosis of cervical metastatic lymph nodes in papillary thyroid carcinoma: Comparison of ultrasound, computed tomography, and combined ultrasound with computed tomography. Thyroid 18: 411-418, 2008.
24. Cho SJ, Suh CH, Baek JH, Chung SR, Choi YJ and Lee JH: Diagnostic performance of CT in detection of metastatic cervical lymph nodes in patients with thyroid cancer: A systematic review and meta-analysis. Eur Radiol 29: 4635-4647, 2019.
25. Haugen BR, Alexander EK, Bible KC, Doherty GM, Mandel SJ, Nikiforov YE, Pacini F, Randolph GW, Sawka AM, Schlumberger M, *et al*: 2015 American thyroid association management guidelines for adult patients with thyroid nodules and differentiated thyroid cancer: The American thyroid association guidelines task force on thyroid nodules and differentiated thyroid cancer. Thyroid 26: 1-133, 2016.
26. Alhassan R, Al Busaidi N, Al Rawahi AH, Al Musalhi H, Al Muqbali A, Shanmugam P and Ramadhan FA: Features and diagnostic accuracy of fine needle aspiration cytology of thyroid nodules: Retrospective study from Oman. Ann Saudi Med 42: 246-251, 2022.
27. Wang H, Zhao S, Yao J, Yu X and Xu D: Factors influencing extrathyroidal extension of papillary thyroid cancer and evaluation of ultrasonography for its diagnosis: A retrospective analysis. Sci Rep 13: 18344, 2023.
28. Guerrini S, Bagnacci G, Perrella A, Meglio ND, Sica C and Mazzei MA: Dual energy CT in oncology: benefits for both patients and radiologists from an emerging quantitative and functional diagnostic technique. Semin Ultrasound CT MR 44: 205-213, 2023.

29. Han A, Liu Y, Cai L, Xie J and Hu S: The diagnostic performance of dual-energy CT imaging in cervical lymph node metastasis of papillary thyroid cancer: A meta-analysis. Front Med (Lausanne) 11: 1457307, 2024.
30. Tunlayadechanont P and Sananmuang T: Dual-energy CT in head and neck applications. Neuroradiol J: 19714009251313507, Jan 8, 2025 (Epub ahead of print).
31. Zhou L, Zhu Q, Yao J, Yang C and Xu D: Correlation analysis of nodular sonographic parameters with cervical lymph node metastases in papillary thyroid carcinoma. Biomed Res Int 2022: 4680064, 2022.
32. Ren J, Liu B, Zhang LL, Li HY, Zhang F, Li S and Zhao LR: A taller-than-wide shape is a good predictor of papillary thyroid carcinoma in small solid nodules. J Ultrasound Med 34: 19-26, 2015.
33. Vaish R, Mahajan A, Sable N, Dusane R, Deshmukh A, Bal M and D'cruz AK: Role of computed tomography in the evaluation of regional metastasis in well-differentiated thyroid cancer. Front Radiol 3: 1243000, 2023.
34. Geng D, Zhou Y, Shang T, Su GY, Lin SS, Si Y, Wu FY and Xu XQ: Effect of Hashimoto's thyroiditis on the dual-energy CT quantitative parameters and performance in diagnosing metastatic cervical lymph nodes in patients with papillary thyroid cancer. Cancer Imaging 24: 10, 2024.
35. Zhang L, Li Y, Chen Z, Dai X, Gao H and Chen Y: Diagnostic performance of dual-energy computed tomography (DECT) quantitative parameters for detecting metastatic cervical lymph nodes in patients with papillary thyroid cancer: A systematic review and meta-analysis. Eur J Radiol 183: 111917, 2025.
36. Yoon J, Choi Y, Jang J, Shin NY, Ahn KJ and Kim BS: Preoperative assessment of cervical lymph node metastases in patients with papillary thyroid carcinoma: Incremental diagnostic value of dual-energy CT combined with ultrasound. PLoS One 16: e0261233, 2021.
37. Santos Armentia E, Martín Noguerol T, Silva Priegue N, Delgado Sánchez-Gracián C, Trinidad López C and Prada González R: Strengths, weaknesses, opportunities, and threat analysis of dual-energy CT in head and neck imaging. Radiologia (Engl Ed) 64: 333-347, 2022.